Functional regulation of BK potassium channels by γ1 auxiliary subunits

Vivian Gonzalez-Perez, Xiao-Ming Xia, and Christopher J. Lingle[1]

Department of Anesthesiology, Washington University School of Medicine, St. Louis, MO 63110

Edited by Richard W. Aldrich, The University of Texas at Austin, Austin, TX, and approved February 20, 2014 (received for review November 25, 2013)

Many K^+ channels are oligomeric complexes with intrinsic structural symmetry arising from the homo-tetrameric core of their pore-forming subunits. Allosteric regulation of tetramerically symmetric proteins, whether by intrinsic sensing domains or associated auxiliary subunits, often mirrors the fourfold structural symmetry. Here, through patch-clamp recordings of channel population ensembles and also single channels, we examine regulation of the Ca^{2+}- and voltage-activated large conductance Ca^{2+}-activated K^+ (BK) channel by associated γ1-subunits. Through expression of differing ratios of γ1:α-subunits, the results reveal an all-or-none functional regulation of BK channels by γ-subunits: channels either exhibit a full gating shift or no shift at all. Furthermore, the γ1-induced shift exhibits a state-dependent labile behavior that recapitulates the fully shifted or unshifted behavior. The γ1-induced shift contrasts markedly to the incremental shifts in BK gating produced by 1–4 β-subunits and adds a new layer of complexity to the mechanisms by which BK channel functional diversity is generated.

asymmetry | allostery | Slo1 channels

Large conductance Ca^{2+}-activated K^+ (BK) channels, like most K^+ channels and many other oligomeric protein complexes, exhibit structural symmetry that arises from the homo-tetrameric assembly of four identical pore-forming α-subunits (1–3). Structural symmetry in turn dictates many aspects of the functional behavior of such proteins. For BK channels, activation can occur either by voltage alone or independently by cytosolic Ca^{2+} (4, 5). Activation initiated by voltage arises from independent movements of voltage sensors, one intrinsic to each α-subunit, which then allosterically couple to a conformational change, termed gating, that permits ion permeation through the central axis of the tetrad of subunits (5). For activation by Ca^{2+}, up to two Ca^{2+} binding events per α-subunit are thought to regulate the conformational status of a symmetric cytosolic gating ring (6–8), which then couples to pore opening. The mechanics and energetics of the gating process display a functional symmetry inherent from the independent participation of the sensing domains of each of the identical α-subunits (5).

For BK channels, the pore-forming α-subunits can also associate with members of a family of four β-subunits (β1–β4) that define many tissue-specific properties of BK channels (9, 10), including apparent Ca^{2+} dependence of activation (11, 12), inactivation (12–15), and pharmacology (12, 16). Insight into how such channel-associated proteins modify channel gating properties is therefore critical to understanding the physiological roles of ion channels in their native cellular environment. For BK channels, auxiliary β-subunits associate with α-subunits in an up to 1:1 stoichoimetry (Fig. S1*A*), maintaining the overall symmetry of the ion channel complex (3). However, functional channels can contain less than a full set of four β-subunits (3), contributing to the functional diversity of BK channels in native cells (17). In such cases each individual β-subunit contributes an essentially energetically additive increment to β-subunit–induced shifts in channel gating (3). In contrast, for auxiliary subunits of many Kv channels, it is not clear whether channels with partial auxiliary subunit stoichiometry may occur. Recently, a second family of BK channel auxiliary subunits, now termed γ-subunits (18–20), has been identified. Although both β- and γ1-subunits share an ability to shift activation of BK channels at a given $[Ca^{2+}]$ to more negative voltages, β- and γ-subunits share no structural (Fig. S1*B*) or sequence homology. It has been proposed that γ1-subunits shift BK gating by specifically enhancing voltage-sensor coupling to channel activation, whereas the effects of β-subunits are more complex (8, 18). Here, we address whether γ1-subunits incrementally shift gating in a fashion similar to the incremental effects produced by each β-subunit in a BK channel complex (3). In contrast to β-subunits, we observe that the fundamental unit of γ1-subunit(s) shifts gating in an all-or-none fashion. Although a number of stoichiometric possibilities can account for the γ1-induced gating shifts, these all require that the rules of γ1 assembly or mechanisms of γ1 modulation differ from those previously established for β-subunits. The contrast between the incremental β-subunit effects and all-or-none γ1-subunit effects adds to the diversity of mechanisms available to define BK channel properties.

Results

γ1-Subunits Shift BK Gating in an All-or-None Fashion. Both γ1- and inactivation-removed β2 (β2(ΔFIW))-subunits allow BK channels to be activated at more negative voltages at a given $[Ca^{2+}]$ (Fig. S1*C*). With 10 μM Ca^{2+}, the voltage at which BK channels are half activated (V_h) is shifted by approximately −50 mV for β2(ΔFIW) subunits (Fig. S1*D*) and approximately −120 mV for the γ1-subunit (Fig. S1*D*). Indicative of mechanistic differences in β2 vs. γ1 effects, the γ1-subunit produces a shift in the V_h of the conductance–voltage (GV) curve of approximately −120 mV at 0 Ca^{2+}, whereas β2- (and β1)-subunits produce little change in V_h at 0 Ca^{2+} (Fig. S1*D*). In previous work the fractional occupancy of BK channels by β-subunit was titrated by expression of different mole-fractions of α:β-subunits (3). This revealed that individual BK channels can contain from none to four β-subunits,

Significance

K^+ channels are oligomeric complexes that typically exhibit structural symmetry arising from the homo-tetrameric core of their pore-forming subunits. Allosteric regulation of tetramerically symmetric proteins, whether by intrinsic sensing domains or associated auxiliary subunits, often mirrors the fourfold structural symmetry, as is the case for regulation of large conductance Ca^{2+}-activated K^+ (BK) channels by auxiliary β-subunits. Here we describe an all-or-none regulation of BK channels by auxiliary γ-subunits that requires that a single γ1-subunit (or complex) is sufficient to produce the full regulatory effect. The contrast between incremental gating shifts produced by 1–4 β-subunits and the γ1-induced all-or-none shifts expands the range of mechanisms available to generate functional diversity in BK channels.

Author contributions: V.G.-P. and C.J.L. designed research; V.G.-P. and C.J.L. performed research; X.-M.X. contributed new reagents/analytic tools; V.G.-P. and C.J.L. analyzed data; and V.G.-P. and C.J.L. wrote the paper.

The authors declare no conflict of interest.

This article is a PNAS Direct Submission.

[1]To whom correspondence should be addressed. E-mail: clingle@morpheus.wustl.edu.

This article contains supporting information online at www.pnas.org/lookup/suppl/doi:10.1073/pnas.1322123111/-/DCSupplemental.

each subunit contributing in an energetically independent fashion to shift BK gating (3).

We similarly examined BK currents activated with 10 μM Ca^{2+} in inside-out patches from oocytes in which different ratios of γ1:α message was injected (Fig. 1*A*). For BK channels with high γ1:α-subunit injection ratios (1:1 or greater), the fractional activation of BK channels is largely well described by a simple Boltzmann curve with V_h at 10 Ca^{2+} μM of −93.4 ± 2.8 mV (SEM; Fig. 1*B*). However, in many patches even at high γ1:α ratios, a small component not well described by a single shifted Boltzmann was present (Figs. 1*B*, 3*B*, and 4*C* but not 4*D*). This was also noted in previous work (18). When this unshifted component is included in a two-Boltzmann fit, the V_h for the fully shifted component is −97.7 ± 2.6 mV. For the α-subunit alone, the GV curve is described by a single Boltzmann with V_h = +22.6 ± 3.4 mV. Over a range of intermediate γ1:α ratios, the GV curves are best described by two Boltzmann components, with one component fit with a V_h similar to that with γ1-subunit overexpression and the other characteristic of channels formed from α-subunits alone (Fig. 1*B*). Over the range of tested γ1:α ratios, the measured V_h values correspond to either that of γ1-type channels or that of α-alone channels (Fig. 1*C*), whereas the relative ratio of the two components changes with γ1:α ratio (Fig. 1 *B* and *D*). This behavior is consistent with individual channels either having a single unitary type of shift when affected by γ1-subunits or being unaffected. We consider this behavior as being functionally all-or-none, although this behavior makes no explicit predictions regarding subunit stoichiometry.

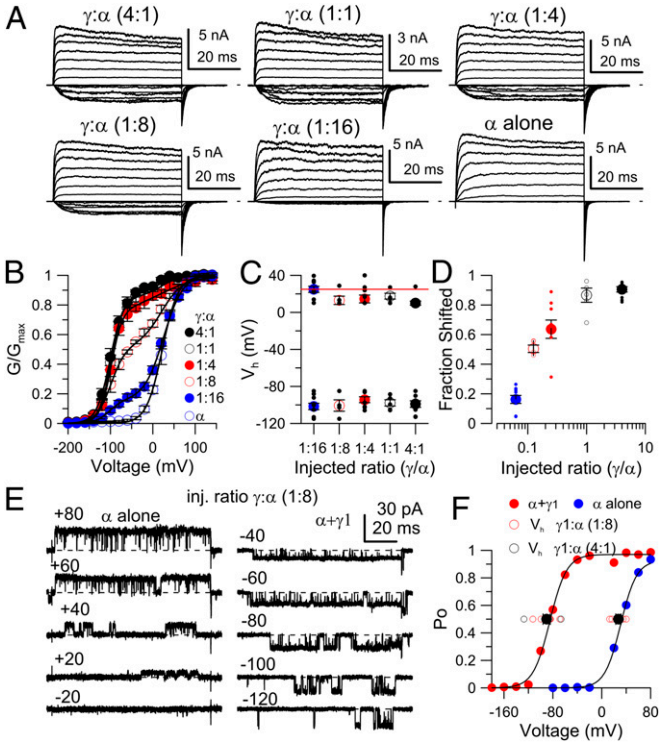

Fig. 1. All-or-none gating shift caused by γ1 (LRRC26) subunit on BK channels. (*A*) Traces show families of currents in symmetrical K^+ with 10 μM cytosolic Ca^{2+} resulting from the indicated injected γ1:α molar ratios. Voltage steps, −200 to +140 mV. (*B*) Tail current GV curves at different injection ratios. Solid lines, fits of a double Boltzmann fit. (*C*) V_h values for each of two Boltzmann components for each injection ratio. Large symbols, means with SEs (SEM). Small symbols, individual patches. Red line, average value for Slo1 alone. (*D*) Mean, SEM, and individual values for fraction of current arising from most shifted component at different injection ratios. (*E*) Representative traces of the activity of a single BK channel recorded in patches from oocytes injected with a 1:8 γ1:α ratio, with activation steps to the indicated voltages with 10 μM Ca^{2+}. (*Left*) Activity for one patch presumably lacking the γ1 shift effect; (*Right*) a channel with the γ1 shift effect. (*F*) Po values for the patches in *E* are plotted vs. membrane voltage with fitted Boltzmann curves (V_h = −85 mV and 31 mV for α+γ1 and α alone, respectively). Solid black circles plot mean V_h values (±SEM) for 10 left-shifted patches (7 for 1:8 γ1:α ratio and 3 for 4:1 γ1:α ratio) and 6 (all 1:8 γ1:α) right-shifted patches, with open symbols showing individual values at the indicated injection ratios.

We next examined single channel open probability (Po) over a range of voltages to obtain a V_h estimate at 10 μM for a set of channels from oocytes injected with a 1:8 γ1:α ratio, a condition for which the ratio of shifted to unshifted channels is approximately 1 (Fig. 1 *B* and *D*). We observed single channels of only two distinct behaviors: one opened at voltages similar to that expected for channels arising from α-subunits alone (Fig. 1*E*, *Left*), and the other activated at much more negative voltages characteristic of γ1-containing channels (Fig. 1*E*, *Right*). The Po-V relationships (Fig. 1*F*) revealed an ∼120-mV difference in V_h for these two channels. The Po-V relationship was defined for a total of 13 patches at 1:8 γ1:α ratio (Fig. 1*F*). Seven patches yielded a mean V_h of −88.7 ± 5.2 mV (SEM) and six patches a mean of 27.2 ± 4.3 mV, a unitary separation of ∼115 mV, consistent with the separation of shifted and unshifted components of the macroscopic GV curves. Three additional patches from oocytes injected with a 4:1 γ1:α ratio showed only shifted Po-V relationships [−93.6 ± 17.8 mV (SEM)]. In no case was a channel of some intermediate shift behavior observed. Thus, the single channel properties support the conclusion that the macroscopic GV curves reflect two populations of channels, one unaffected by the presence of γ1-subunits and one fully shifted by the γ-subunits. We therefore conclude that regulation of BK gating by γ1-subunits occurs in a functionally all-or-none fashion, unlike the effects of β-subunits (3).

That the γ1-induced gating shift occurs in a functionally all-or-none fashion provides no information about γ1:α stoichiometry. We can only conclude that some elementary unit of γ1-subunit(s) is sufficient to produce the gating shift. We envision three general categories of model (Fig. S2) that could produce an all-or-none behavior. In model 1, one to four γ1-subunits can assemble in a channel (as observed for β-subunits), but one is sufficient to produce the full gating effect. In model 2, γ1-subunits are only associated with α-subunits in a fixed stoichiometry, whether involving, for example, one, two, or four γ1-subunits in the unit. This would be similar to Kv β-subunit association with Kv α-subunits (21). In model 3, up to some fixed number of γ1-subunits can assemble in a channel, but only when the full complement (whether two or four) is present in the channel does the gating shift occur.

Both Incremental β-Type and All-or-None γ1-Type Gating Shifts Can Be Accounted for Within the Context of the General Horrigan-Aldrich Allosteric Model. The regulation of macroscopic BK gating can be effectively described by the Horrigan-Aldrich allosteric model (5), in which a central closed–open gating equilibrium (constant L) is regulated, on one hand, by the voltage-sensor equilibrium (constant J with coupling constant D) and, on the other, by coupling to a Ca^{2+} binding equilibrium (constant K, with coupling constant C). To provide a mechanistic framework for evaluation of how partial auxiliary subunit stoichiometries (Fig. S2) may impact on gating shifts, we considered whether incremental vs. all-or-none shifts in gating can be accounted for within the context of the fourfold symmetric Horrigan-Aldrich model (5). To assess the predictive usefulness of the HA formulation, here we first evaluate the situation encapsulated in model 1. Model 1 is guided by previous observations with β-subunits in which mature channels can contain less than a full complement of auxiliary subunits. We assume that up to four auxiliary subunits, whether β or γ1, can assemble in a full BK channel complex. In such a case the distribution of channels among five stoichiometric possibilities is dictated by predictions of binomial assembly for a given ratio of α- and γ1-subunits. For illustrative purposes, we also make the simplification that any

auxiliary subunit effect involves only a single allosteric constant of the HA formulation. We consider two cases. First, in one case, as each subunit assembles in a channel, it incrementally alters a given allosteric constant such that for parameter P for a channel with i auxiliary subunits, $P_i = (P_{min}^{4-i} P_{max}^{i})^{0.25}$, where P_{min} is the allosteric constant with no auxiliary subunits, and P_{max} describes the constant, when a channel is fully occupied by auxiliary subunits. This corresponds to the case that each auxiliary subunit energetically influences a single α-subunit in the tetramer. This is illustrated in Fig. 2*A* for allosteric constant D, which describes coupling between voltage-sensors and channel opening. The effect of the γ1-subunit on BK gating has been proposed to involve an increase in D from 25 to 425 (18). As the mole-fraction of auxiliary subunits within the channel population is increased, the predicted GV curves shift leftward, with intermediate GV curves exhibiting a shallower slope than those with no or four auxiliary subunits. A similar analysis of the effect of incremental effects of an auxiliary subunit involving allosteric constants J, L, and C shows that similar incremental shifts in gating are expected as a function of channel fractional occupancy by the auxiliary subunit (Fig. 2 *C*, *E*, and *G*). This mirrors the effects of β1- and β2-subunits on BK gating as a function of β:α injection ratio (3) but not the behavior of γ1:α injection ratios. The purpose of the analysis here is not to assign the β-subunit mediated gating shifts to a particular set of allosteric constants but to provide a general explanation for how the previously observed incremental shifts in GV curves may be generated within the context of the HA formulation. Second, we consider the case in which association of a single auxiliary subunit with a channel produces a full gating shift. This would represent a case of extreme negative cooperativity (i.e., additional auxiliary subunits produce minimal additional effect on gating). The behavior of GV curves for a population of channels as the mole-fraction of auxiliary subunits is increased is shown in Fig. 2*B*. The two distinct Boltzmann components are obvious, and the properties of the GV curves are comparable to the consequences of expression of different ratios of γ1:α-subunits. An all-or-none alteration in other allosteric constants can also predict inflections in GV curves as a function of injection ratio (Fig. 2 *D*, *F*, and *H*). This analysis establishes, perhaps not surprisingly, that both β and γ1 gating shifts can be readily accounted for within the HA context.

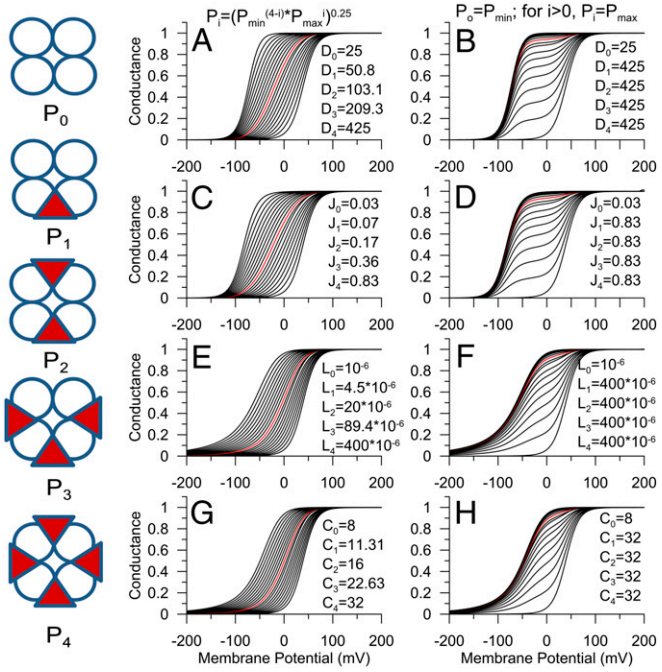

Fig. 2. Both incremental and all-or-none gating shifts can be explained within the context of the HA model. (*Left*) Diagrams reflect five potential γ1:α-subunit stoichiometries: triangles, γ1-subunits; circles, α-subunits. P_i reflects the value of a given allosteric parameter for that particular stoichiometry (P_{0-4}), with the value defined from equations on the top. (*A*, *C*, *E*, and *G*) Incremental changes in a given overall allosteric constant; (*B*, *D*, *F*, and *H*) all-or-none effects. For all panels, each curve corresponds to a different mole fraction of modified subunits (p_i = 0–1, stepsize 0.05). Red curve corresponds to p_i = 0.5. For a given p_i, conductance was calculated based on an HA model for a population of channels with stoichiometries defined by expected binomial distribution expected for a given p_i. Default HA parameters were L = 10^{-6}, D = 25, J = 0.03, C = 8, K = 11, E = 2.4, with z_L = 0.3*e* and z_J = 0.58*e*, with $[Ca^{2+}]$ = 10 μM. (*A*) Values of D for different stoichiometries were calculated from the indicated equation with D_{min} = 25 and D_{max} = 425. (*B*) A single active subunit was sufficient to make D for any subunit combination 425. (*C*) J was varied incrementally for each stoichiometric combination. (*D*) J was varied in an all-or-none fashion. (*E*) L was varied in an incremental fashion. (*F*) L was varied in an all-or-none fashion. (*G*) C was varied incrementally. (*H*) C was varied in an all-or-none fashion.

Changes in Shifted/Unshifted Ratio Do Not Unambiguously Distinguish Among Models. Although the above analysis focuses on model 1 to illustrate how a functionally all-or-none gating shift might arise, an all-or-none effect might arise from two other general stoichiometric possibilities, models 2 and 3 (Fig. S2). To assess whether a given model might be more consistent with the observed variation in fraction of shifted channels as a function of γ1:α injection ratio, we calculated predicted GV curves (Fig. S3) based on different stoichiometric ratios of γ1:α-subunits for each model (Fig. S2). The GV curves derived from each model (Fig. S3) reveal distinct differences in the amount by which the shifted/unshifted ratio changes as the mole-fraction of γ1-subunits is increased. Thus, if we assume for the moment that the mole-fraction of γ1-subunits that assembles into functional BK channels varies with α-subunits in a linear fashion based on the γ1:α injection ratio, the different models make distinct predictions for how steeply the fraction of shifted channels should vary with injection ratio (Fig. S4*A*). This can then be compared with the actual data (Fig. S4*B*). The different models make different predictions for how the slope of the gating shift/fractional occupancy relationship varies. For model 1, increases in occupancy produce a gradually saturating increase in gating shift. For model 2, gating shifts vary linearly with increases in occupancy, whereas model 3 predicts a superlinearity. If one compares the experimental data with models 1 and 2 (Fig. S4*C*) assuming a direct equivalence of injection ratio and fractional occupancy, this suggests that model 1 is more consistent with the variation in gating shift with injection ratio. However, the challenge in this analysis is that true fractional occupancy does not necessarily directly correlate with the γ1:α injection ratio. As an alternative assumption regarding the relationship between fractional occupancy and injection ratio, it can be recognized that the minimal observed fractional shift of 0.17 observed at the 1:16 γ1:α ratio (Fig. S4*B*, dotted line) corresponds in a given model to a specific fractional occupancy (as indicated by the dotted line in Fig. S4*A*). This allows renormalization of the injection ratio data in terms of fractional occupancy for different models (Fig. S4*D*) and suggest that both models 1 and 2 capture the general trends of the observed values. An unexplained aspect of our results is that, even at the highest injection ratios, an unshifted component of current is generally observed. Overall, given scatter in the data, the change in the fractional shift as a function of injected γ1:α ratio does not readily distinguish between models 1 and 2, whereas model 3 is unlikely (Fig. S4*D*).

Model 1 represents a limiting case of negative cooperativity: each additional γ1-subunit has no additional impact on gating. For a GV shift occurring in accordance with model 1, we wondered to what extent GV shifts such as those in Fig. 1 might be explained by a case in which the effect of a single γ1-subunit was not completely all-or-none but some fraction of a full effect. We tested cases in which a single γ1-subunit produced various fractions (0.5–1.0) of a full-shift effect (Fig. S5 *A–D*). This analysis leads to the conclusion that the experimental measurements

(Fig. 1 *C* and *D*) are largely indistinguishable from a full all-or-none gating shift. However, a full shift can probably not be distinguished from a single γ1-subunit producing an effect of 0.8 or greater of a full effect, for which less than a 10-mV shift in the shifted V_h component is predicted (Fig. S5 *E* and *F*). Even in such a case, a single subunit would be producing almost a full effect on the GV. On balance, with the assumption that model 1 is applicable, these considerations indicate that the effect of a single γ1-subunit would be largely consistent with complete negative cooperativity (i.e., all-or-none).

The All-or-None γ1 Shift Effect is Labile. An intriguing aspect of the γ1 effect is that, under some conditions, the γ1-induced shift in BK gating diminishes with time after patch excision (Fig. 3*A*). For this type of experiment, a GV curve was generated immediately after excision with 10 μM Ca^{2+}. Subsequently, additional GV curves were generated at 10 μM Ca^{2+}, with intervening exposures (usually 2 min) to 0 Ca^{2+} (Fig. 3 *A* and *B*). As time after patch excision increased, the single fully shifted Boltzmann that was initially observed after patch excision split into two components, one generally characteristic of γ1-shifted channels and one characteristic of α-alone channels. With sufficient elapsed time, the GV curve approached a single Boltzmann characteristic of a population of channels unaffected by a γ1-subunit (Fig. 3*B*). Although the GV curves during this run-down clearly exhibited inflection points consistent with the presence of shifted and unshifted channel populations, we noticed that immediately after patch excision there was an initial rightward shift in the GV, which was not associated with the appearance of an unshifted fraction. With additional time, as distinctly separate components appeared in the GV curves, the curves could be well fit with a two-component Boltzmann function, but the separation between fully shifted and unshifted fractions (Fig. S6*A*) was not as well defined as for the GV curves obtained from defined ratios of injected γ1/α-subunits. A plot of the V_h of the negatively shifted component as a function of time revealed an approximately +20- to 30-mV rightward shift occurring in the first 2 min after excision (Fig. S6*B*), which does not undergo any additional shift as the fraction of the shifted component decreases. Therefore, this early GV change, whatever its basis, seems to be largely complete before the subsequent large gating shift. Despite this early shift behavior, the subsequent more prominent (~100 mV) full loss of the γ1-mediated gating shift, as evidenced by the split into two components in the GV curves, recapitulates the all-or-none effect demonstrated with injections of different ratios of γ1:α-subunits. We postulate that the major component of the run-down process involves a conversion of an active γ1-subunit(s) to an inactive form that no longer has an effect on BK gating. We considered the possibility that, if channels do contain more than 1 γ1-subunit, perhaps the early gating shift might reflect some initial change in effect of a γ1-subunit, before a final loss of effect. However, if that were the case, in our titration experiments the shifted V_h would have varied at least 20–30 mV between the 1:8 and 4:1 γ1:α injection ratios. This was not observed.

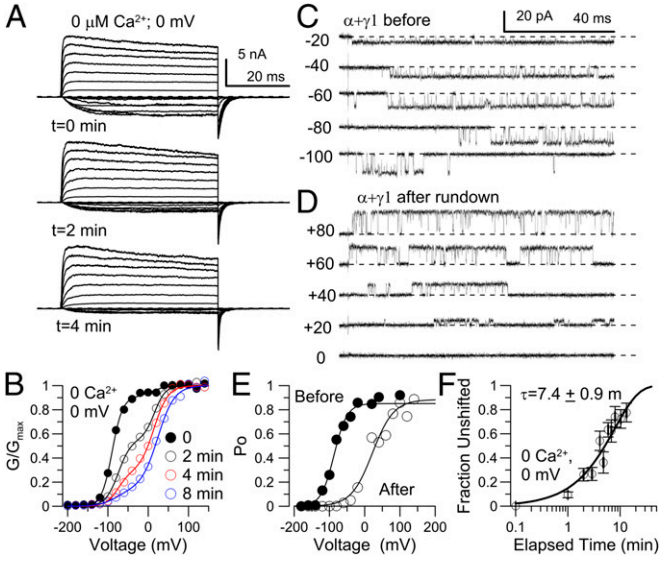

Fig. 3. The γ1-induced shift effect is labile. (*A*) Patch was held in 0 Ca^{2+}, 0 mV. At 0, 2, and 4 min, 10 μM Ca^{2+} was applied and the illustrated families of traces were obtained. Voltage steps, −200 to +140 mV. (*B*) GV curves from traces as in *A*, with lines reflecting two Boltzmann fits. (*C*) A single α+γ1 channel activated by steps to the indicated voltages (with 10 μM Ca^{2+}). (*D*) For the same channel in *C*, after 2 min in 0 Ca^{2+} solution, the channel underwent an abrupt change in Po. (*E*) Po-V curves determined for the patch shown in *C* and *D*, with V_h values indicated. (*F*) The fraction of unshifted component from a two-Boltzmann fit to the GV curves as in *B* is plotted as a function of elapsed time for all patches.

To confirm that the two component Boltzmann curves observed during run-down reflect a conversion from fully shifted to unshifted channels, we examined the behavior of single channels during run-down (Fig. 3 *C* and *D*). A Po-V relationship was initially determined in 10 μM Ca^{2+} after patch excision (Fig. 3 *C* and *E*). V_h for the illustrated channel was initially −87 mV. Po-V was again determined in 10 μM Ca^{2+} after 2-min periods in 0 Ca^{2+}. For this patch, after 2 cumulative minutes in 0 Ca^{2+}, the channel underwent (Fig. 3 *D* and *E*) a large change in Po at a given voltage with a new V_h of +22 mV. Similar step changes in Po were observed for a total of four other channels, although in each case the step change followed different cumulative exposure times in 0 Ca^{2+}. One two-channel patch exhibited a stepwise shift in gating, with the time of the shift different for the two channels. For a set of four single channels, we observed a step-change from a Po_{50} of −90.8 ± 6.6 mV to +27 ± 7.1 mV (Fig. 3*E*), the latter value being indistinguishable from the V_h for channels arising from α-subunits alone. We conclude that the run-down in the γ1-mediated gating shift also reflects largely an all-or-none effect (i.e., γ1-subunits undergo a conversion from a fully active to a fully inactive status). We postulate that the initial alteration that is observed after excision may reflect an intermediate γ1 condition in which its effect on allosteric D is partially diminished. As will be shown below, manipulations that impeded run-down also prevent the occurrence of the initial small V_h shift, suggesting that both are part of changes in the status of the γ1-subunits. Thus, the lability of the γ1-mediated effect indicates that individual channels either retain the full γ1-mediated shift or are not shifted at all. This is again consistent with models in which one γ1-subunit or complex of γ1-subunits is largely sufficient to produce the shift effect. Although we observed that openings of single α+γ1-channels exhibited reduced single channel conductance (Fig. S7*A*) and an increased occurrence of subconductance excursions compared with openings of α alone channels (Fig. S7 *B* and *C*), we have not noted any features of single channel openings that might be informative about the number of γ1-subunits that may be present in a channel. Intriguingly, the subconductance excursions persisted in channels for which the γ1-mediated shift effect had disappeared (Fig. S7*D*), suggesting that γ1-subunits remain associated with the BK complex, despite the loss of the shift effect. On the basis of the averaged time course of increase in the unshifted channel population, the γ1-mediated shift effect decays with a time constant of ~7 min (Fig. 3*F*).

The Run-Down of the γ1-Mediated Shift Is State Dependent and Slowed in Open States. The lability of the γ1-induced gating shift requires that all or most α+γ1-channels are fully shifted when present in the intact oocyte membrane. Although a complete analysis of the run-down effect will require extensive investigation beyond this report, we tested the impact of several factors on the time course of run down. First, the run-down of

the γ1-mediated effect was markedly slowed or absent in patches continuously bathed in 10 μM Ca^{2+} (Fig. 4 *A*, *C*, and *E*). This might arise either from an effect of Ca^{2+} or from state-dependent inhibition of run-down. At 10 μM Ca^{2+} and 0 mV, α+γ1-channels are open almost all of the time. We therefore examined rundown in patches bathed with 0 Ca^{2+}, but held at +80 mV, also maintaining channels primarily in open states (Fig. 4 *B*, *D*, and *F*). This also slowed channel run-down. We conclude that the transition of γ1-subunits from active to inactive is hindered when BK channels are maintained in the open conformation. The inhibition of run-down also abolished the initial rightward shift in the GV curves observed during the first 2 min in 0 Ca^{2+} conditions, supporting the idea that the initial rightward shift is also associated with some change in γ1-subunit status that is a prelude to the full all-or-none loss of effect on BK gating. We wondered whether the run-down might reflect some loss of some constituent of the cytosol or membrane that was hindered in a state-dependent fashion. We therefore tested the ability of various factors to influence the loss of the α+γ1 gating shift. Phosphatidylinositol-bisphosphate (PIP_2; 10–25 μM), either as C8-PIP2, C16-PIP, or native brain PIP_2, neither slowed the run-down time course nor restored the γ1 effect. Similarly, 5 mM ATP did not influence run-down measured at 0 mV, 0 Ca^{2+}.

The Time Course of Run-Down Exhibits a Delay. The time-course of the run-down may reflect a change in γ1-subunit(s) from an active, shift-inducing form to an inactive form. Given that the effect is all or none, if a single γ1-subunit or single complex of γ1-subunits must become inactive to cause the loss of gating shift, the time course should exhibit a single exponential time course.

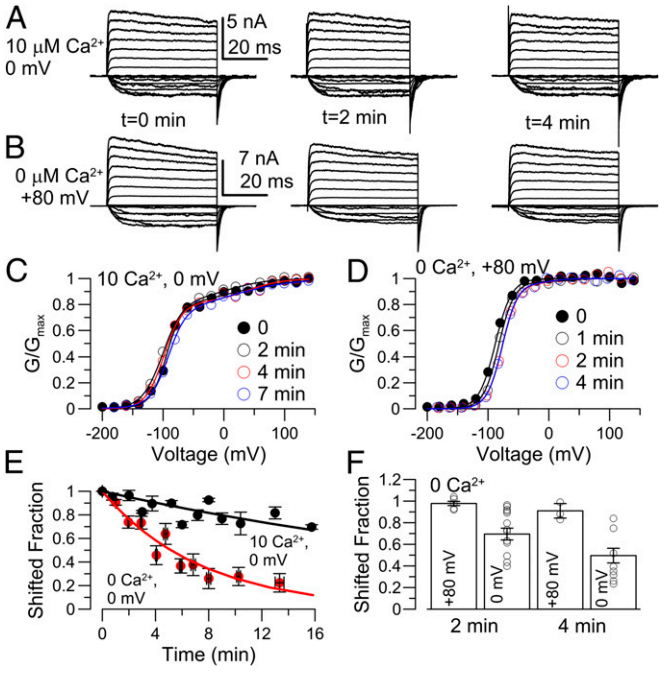

Fig. 4. Loss of γ1-induced gating shift is hindered in a state-dependent fashion. (*A*) After patch excision, the patch was held at 10 μM Ca^{2+}, 0 mV for the indicated cumulative time between each family of traces (left to right). (*B*) Patch was held at 0 Ca^{2+}, +80 mV between families of traces (GVs at 10 μM Ca^{2+}). (*C*) GV curves from traces in *A*. (*D*) GV curves from traces in *B*. (*E*) The fraction of the most negatively shifted GV component in a two-Boltzmann fit is plotted vs. elapsed time at 0 Ca^{2+}, 0 mV (Fig. 3) and for 10 μM Ca^{2+}, 0 mV (as in *A*). Values from individual patches were averaged over segments of time. Single exponential time constant of loss of shift was 7.4 min in 0 Ca^{2+} and, for 10 μM Ca^{2+}, 39.5 min. (*F*) Means and individual values of loss of shift are plotted for 2 and 4 min after patch excision, revealing some variability among patches in rundown at 0 mV, 0 Ca^{2+}.

If up to four γ1-subunits must sequentially become inactive before the gating shift disappears, the time course might exhibit a lag reflecting the number of initially active subunits. We measured the time course of the increase in the unshifted component, because this minimizes complexities that might arise from the contribution of the initial 20-mV rightward GV shift (Fig. S6). For individual patches, we fit the increase in the fraction of the unshifted population of channels with $f(t) = [1 - \exp(-t/\tau)]^n$, where τ is the time constant of the active to inactive conversion of a single γ1-subunit, and n is the number of subunits involved. Of a set of six patches, three patches exhibited a time course of run-down generally consistent with a single exponential time course, whereas three exhibited run-down better described with a delay in the range of $n = 3$–4 (Fig. S8*A*). However, the intrinsic τ for five of the six patches in this set was essentially identical (4.6 ± 0.7 min), with only the apparent stoichiometry differing (Fig. S8*B*). If the intrinsic stoichiometry varies to some extent among patches because of differences in γ1 expression, this might explain some of the variability in the run-down time course. However, at present we cannot explain why, at identical injection ratios, we are unable to consistently drive the apparent stoichiometry to full saturation such that $n = 4$. As noted earlier, in most patches, we generally observed some initial small unshifted component, even at the highest γ1:α injection ratios. On the basis of this, consideration of Fig. 1 indicates that, even for a population of channels that are well over 90% shifted, the average number of γ1-subunits per channel may still only be in the range of 1.5–2.5. We therefore suggest that full stoichiometric assembly has not been achieved consistently in our experiments, perhaps a limitation of the oocyte system. Irrespective of these complexities, the up to $n = 3$–4 lag observed in the onset of the loss of the γ1 gating shift in some patches would be consistent with the idea that more than one γ1-subunit can coassemble with BK α-subunits. Alternatively, such a delay might arise from some other additional component of the system that regulates γ1 function, but also involving a fourfold stoichiometry or a four-step process. Alternative methodologies will be required to resolve the issue of γ1:α-subunit stoichiometry.

Discussion

The present results establish that the γ1-subunit shifts BK gating in an all-or-none fashion. Whatever the fundamental unit of γ1 interaction with a BK α-subunit tetramer, that unit produces an approximately −120-mV leftward shift in the activation V_h. This contrasts markedly with the effects of BK β-subunits, for which each of the up to four β-subunits in a BK channel complex incrementally shifts gating (3). Incremental effects on gating, whether by auxiliary subunits or other regulatory processes such as phosphorylation, would be expected to arise naturally from the fourfold symmetry inherent in a tetrameric K^+ channel (i.e., the full channel provides a scaffold of four identical interaction surfaces or four sites for modulation). In contrast, irrespective of the underlying γ1:α stoichiometry, the γ1 shift involves a single unitary effect: channels are either shifted or unshifted. Both types of BK auxiliary subunit effects, incremental or all-or-none, can be usefully described within the context of a now-standard model of BK channel gating. Whatever the stoichiometric basis of the γ1-subunit effects, the contrast between γ1- and β-subunit induced shifts indicates that the energetic consequences of their participation in BK channels are determined in distinctly different ways.

The present experiments do not provide a definitive test of γ1:α stoichiometry or whether partial γ1:α stoichiometries occur. Although the lag in the time course of run-down of the γ1-induced shift effect raises the possibility that up to four γ1-subunits may participate, this test alone is not robust enough to allow any strong conclusion and is also subject to alternative explanations. We envision three primary possibilities. One, as in model 1, is that, similar to the β:α-subunit rules of assembly, none to four γ1-subunits may coassemble in a BK complex, but, in contrast to the incremental β-subunit effects, only one γ1-subunit is sufficient to produce a full gating shift. This scheme maintains structural

symmetry in the channel complex but poses an interesting challenge: how might a single subunit exert an essentially concerted effect to alter the coupling between voltage-sensor and channel opening for all four α-subunits? A second possibility is that only one γ1-subunit assembles in a BK channel complex to produce the full functional effect. Third, perhaps like auxiliary subunits of Kv channels, channels with γ1-subunits may only contain a full set of four γ1-subunits. In general, β-subunits of the Kv1 subunit family (21) and the KChIP subunits that interact with Kv4 α-subunits (22) seem to assemble in an obligatory tetrameric rosette associated with the Kv channel complex (23). In such cases the auxiliary subunit complex would only be expected to confer a full maximal effect. For γ1:α, our results do not adequately distinguish among any of the above three possibilities.

An intriguing observation in our experiments was the lability of the γ1-subunit gating shift. Such a shift was not previously observed in regard to γ1-subunit action, which may reflect differences in cell systems [oocytes vs. HEK and prostate tumor cell lines (18)]. However, the hSlo3 K^+ channel, when coexpressed in oocytes with its γ2-subunit partner [LRRC52 (19)], also exhibits a run-down of similar time course (24). Whether the run-down of Slo3 involves a similar gating shift or a loss of channels is not clear. Given the robust magnitude of the gating shift produced by the γ1-subunits, any endogenous process that regulated the ability of γ1-subunits to produce a gating shift would have a profound effect on the resting conductance of any cells containing such channels. However, in the intact oocyte membrane, the γ1-mediated shift must be largely intact, and it may be that whatever maintains the γ1-shift effect within a native cell is not a process subject to dynamic regulation. Our tests excluded two potential possibilities: the role of PIP_2 and a role for cytosolic ATP. Whether run-down reflects an aspect of γ1 function that can be dynamically regulated remains a topic for future investigation.

In sum, our results describe a functionally all-or-none effect of the γ1 auxiliary subunit on the otherwise symmetric BK channel tetramer. This contrasts markedly to the incremental effects exerted by BK β-subunits. The results are consistent with the major energetic effects of the γ1-subunit arising from either a single γ1-subunit or single complex of γ1-subunits. Additional tests are required to define definitively γ1:α stoichiometry in BK channels.

Materials and Methods

Constructs and Oocyte Expression. Stage IV *Xenopus laevis* oocytes were used for expression. Primary constructs were mSlo1 (7) and human LRRC26 (γ1) (19). β2(ΔFIW) was a construct with the residues 2–4 (FIW) deleted from the N terminus as described previously (25). For functional studies of channels expressed in *Xenopus* oocytes, γ1 RNA was typically injected with Slo1 RNA at specific molar ratios indicated on the figures, and oocytes were used 2–5 d after injection.

Electrophysiology. Gigaohm seals were formed in frog Ringer (in mM: 115 NaCl, 2.5 KCl, 1.8 $CaCa^{2+}$, and 10 Hepes, pH 7.4). The pipette/extracellular solution was (in mM) 140 K-methanesulfonate, 20 KOH, 10 Hepes, and 2 $MgCl_2$, pH 7.0. Macroscopic and single channel currents were typically recorded in the inside-out patch configuration, allowing prefusion of the cytosolic face of the membrane. Preparation of solutions of different Ca^{2+} was as previously described (7) with 140 mM methanesulfonate, 20 mM KOH, 10 mM Hepes, 5 mM EGTA, and pH adjusted to 7.0. Solutions were applied directly to patches via a large-bore pipette tip containing multiple independent solution lines with solution exchange occurring within less than 1 s. Current waveforms were analyzed with Clampfit or software developed within this laboratory. All error bars correspond to SEM. Experiments were at ~22–25 °C. Chemicals were obtained from Sigma (St. Louis, MO). Standard molecular biology methods (7, 12), methods of expression in *Xenopus* oocytes and electrophysiological methods (3, 7, 19) were used. Additional details pertinent to measurement and analysis of gating shifts and predictions of different models of subunit stochioimetry are in *SI Materials and Methods*.

ACKNOWLEDGMENTS. This work was supported by National Institutes of Health Grant GM-081748 (to C.J.L.) and National Research Service Award GM103138 (to V.G.-P.).

1. Shen KZ, et al. (1994) Tetraethylammonium block of Slowpoke calcium-activated potassium channels expressed in *Xenopus* oocytes: Evidence for tetrameric channel formation. *Pflugers Arch* 426(5):440–445.
2. Goodsell DS, Olson AJ (2000) Structural symmetry and protein function. *Annu Rev Biophys Biomol Struct* 29:105–153.
3. Wang YW, Ding JP, Xia XM, Lingle CJ (2002) Consequences of the stoichiometry of Slo1 α and auxiliary β subunits on functional properties of large-conductance Ca2+-activated K+ channels. *J Neurosci* 22(5):1550–1561.
4. Horrigan FT, Cui J, Aldrich RW (1999) Allosteric voltage gating of potassium channels I. Mslo ionic currents in the absence of $Ca^{(2+)}$. *J Gen Physiol* 114(2):277–304.
5. Horrigan FT, Aldrich RW (2002) Coupling between voltage sensor activation, Ca^{2+} binding and channel opening in large conductance (BK) potassium channels. *J Gen Physiol* 120(3):267–305.
6. Schreiber M, Salkoff L (1997) A novel calcium-sensing domain in the BK channel. *Biophys J* 73(3):1355–1363.
7. Xia XM, Zeng XH, Lingle CJ (2002) Multiple regulatory sites in large-conductance calcium-activated potassium channels. *Nature* 418(6900):880–884.
8. Hoshi T, Pantazis A, Olcese R (2013) Transduction of voltage and Ca2+ signals by Slo1 BK channels. *Physiology (Bethesda)* 28(3):172–189.
9. Orio P, Rojas P, Ferreira G, Latorre R (2002) New disguises for an old channel: MaxiK channel beta-subunits. *News Physiol Sci* 17:156–161.
10. Orio P, et al. (2006) Structural determinants for functional coupling between the beta and alpha subunits in the Ca^{2+}-activated K^+ (BK) channel. *J Gen Physiol* 127(2): 191–204.
11. McManus OB, et al. (1995) Functional role of the beta subunit of high conductance calcium-activated potassium channels. *Neuron* 14(3):645–650.
12. Xia X-M, Ding JP, Lingle CJ (1999) Molecular basis for the inactivation of Ca^{2+}- and voltage-dependent BK channels in adrenal chromaffin cells and rat insulinoma tumor cells. *J Neurosci* 19(13):5255–5264.
13. Wallner M, Meera P, Toro L (1999) Molecular basis of fast inactivation in voltage and Ca^{2+}-activated K^+ channels: A transmembrane beta-subunit homolog. *Proc Natl Acad Sci USA* 96(7):4137–4142.
14. Xia XM, Ding JP, Zeng XH, Duan K-L, Lingle CJ (2000) Rectification and rapid activation at low Ca^{2+} of Ca^{2+}-activated, voltage-dependent BK currents: Consequences of rapid inactivation by a novel β subunit. *J Neurosci* 20(13):4890–4903.
15. Uebele VN, et al. (2000) Cloning and functional expression of two families of beta-subunits of the large conductance calcium-activated K^+ channel. *J Biol Chem* 275(30): 23211–23218.
16. Meera P, Wallner M, Toro L (2000) A neuronal beta subunit (KCNMB4) makes the large conductance, voltage- and Ca^{2+}-activated K^+ channel resistant to charybdotoxin and iberiotoxin. *Proc Natl Acad Sci USA* 97(10):5562–5567.
17. Ding JP, Li ZW, Lingle CJ (1998) Inactivating BK channels in rat chromaffin cells may arise from heteromultimeric assembly of distinct inactivation-competent and non-inactivating subunits. *Biophys J* 74(1):268–289.
18. Yan J, Aldrich RW (2010) LRRC26 auxiliary protein allows BK channel activation at resting voltage without calcium. *Nature* 466(7305):513–516.
19. Yang C, Zeng XH, Zhou Y, Xia XM, Lingle CJ (2011) LRRC52 (leucine-rich-repeat-containing protein 52), a testis-specific auxiliary subunit of the alkalization-activated Slo3 channel. *Proc Natl Acad Sci USA* 108(48):19419–19424.
20. Yan J, Aldrich RW (2012) BK potassium channel modulation by leucine-rich repeat-containing proteins. *Proc Natl Acad Sci USA* 109(20):7917–7922.
21. Gulbis JM, Zhou M, Mann S, MacKinnon R (2000) Structure of the cytoplasmic beta subunit-T1 assembly of voltage-dependent K^+ channels. *Science* 289(5476):123–127.
22. Wang H, et al. (2007) Structural basis for modulation of Kv4 K^+ channels by auxiliary KChIP subunits. *Nat Neurosci* 10(1):32–39.
23. van Huizen R, Czajkowsky DM, Shi D, Shao Z, Li M (1999) Images of oligomeric Kv beta 2, a modulatory subunit of potassium channels. *FEBS Lett* 457(1):107–111.
24. Leonetti MD, Yuan P, Hsiung Y, Mackinnon R (2012) Functional and structural analysis of the human SLO3 pH- and voltage-gated K^+ channel. *Proc Natl Acad Sci USA* 109(47):19274–19279.
25. Xia XM, Ding JP, Lingle CJ (2003) Inactivation of BK channels by the NH_2 terminus of the β2 auxiliary subunit: An essential role of a terminal peptide segment of three hydrophobic residues. *J Gen Physiol* 121(2):125–148.